JARÐFEINGI
FAROESE GEOLOGICAL SURVEY

Modelling of the heat dynamics of a geothermal well at Umhvørvisstovan

This report was made on behalf of

Faroese Environment agency

(Umhvørvisstovan)

umhvørvisstovan

as part of the project

SMARTrenew

(Smarter renewable energy and heating Management for Arctic and northern Rural Territories)

funded by

NPA

(Northern Periphery and Arctic program).

smartrenew

Northern Periphery and Arctic Programme 2014-2020

EUROPEAN UNION

Investing in your future
European Regional Development Fund

Content

Abstract 3
Introduction 4
Measurements 5
Introduction to study area 5
Heat recovery from steady state conditions 7
Heat storage experiments 9
3D numerical modelling 12
Initial parameters 13
Boundary conditions 14
Modelling geothermal well 14
Modelling results 16
Model grid 16
Heat recovery experiment 16
Heat storage experiment 18
Conclusion on modelling performance 21
Future work 22
References 23
Appendix A 24
3D numerical modelling 24
Instability criterion 26

Written and compiled by:

Uni K. Petersen, Óluva Eidisgaard, Barbara B. Hansen, Jana Ólavsdóttir

Abstract

One of the largest challenges the Faroese communities face today is how to store the excess energy which is mainly produced from fluctuating wind power. The main aim of this project is to investigate the possibility to store energy in the Faroese basalts, which, if successful would be one sustainable way to store excess energy for later usage.

Based on measurements from a geothermal well prepared for experiments, parameters for a 3D numerical model for heat dynamics in the subsurface are determined.

The 3D modelling is verified to model the heat recovery of the well during one week of measurements, after one year of consumption. Further, modelling of short-term heat response, of varying operation conditions during 3 weeks, are verified by measurements.

Determining the parameters for geothermal modelling is the first step in modelling storing of excess electric power. This is of great importance since experiments with high-temperature wells are not feasible due the large amount of energy needed to raise the temperature significantly.

Introduction

The Faroe Islands is approximately 1,400 km^2 and the population is approximately 53,000 people. The inhabitants in the islands mostly live in private houses in small communities where the majority of the houses use oil boilers as the heating source. The islands have a vision to transform all energy use on land from oil to renewables. The islands have world record conditions for producing electricity from wind and most energy use will thus be based on electric power. Transforming space heating form oil to renewables is seen as a low hanging fruit as electric heat pumps are a proven technology for heating.

Since 2008 the usage of especially ground source heat pumps has increased on the islands and today over 1000 ground source heat pumps utilizing shallow geothermal heat are operating and producing energy for the Faroese homes. Jarðfeingi has measured over 700 of these shallow geothermal boreholes during especially the last four years. These measurements have given a good overview of the geothermal gradient in areas of the islands. These gradients vary from 2,0 °C/m to almost 7 °C/m.

One of the largest challenges the Faroese communities face today is how to store the excess energy which is mainly produced from fluctuating wind power. This study will focus on how the heat flow in a shallow geothermal borehole is affected by the usage of the borehole by doing a row of tests described below.

The main aim is to investigate the possibility to store energy in the Faroese basalts, which, if successful would be one sustainable way to store excess energy for later usage.

Measurements

Introduction to study area

The heating of Umhvørvisstovan is based on a shallow geothermal energy system utilized through the circulation of closed loop brine in four geothermal wells (Figure 1). All wells are at ~43 m elevation. Wells 1, 2, and 4 are 260 m deep while well 3 is 400 m deep.

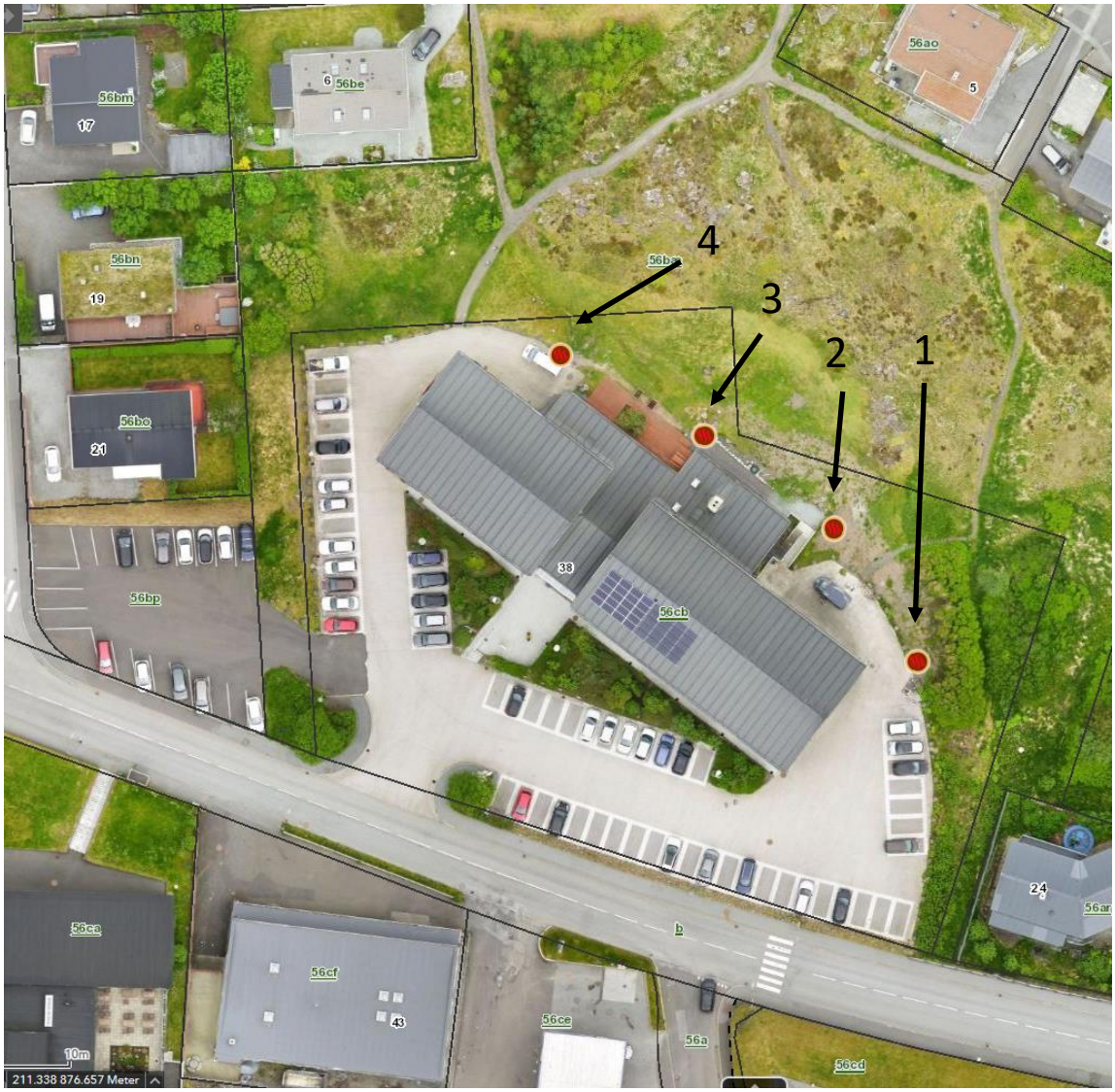


Figure 1. Aerial photo showing Umhvørvisstovan. Arrows show the four geothermal wells. Well number 3 is the one used for the experiment.

After drilling, the temperature profiles of wells 1, 2, and 4 were measured. Wells 1 and 2 were measured on the 17th of November in 2020, while well 4 was measured on the 19th of November in 2020. However, the mounting of the pipes in well 3 immediately after drilling hindered measurements of this well (Figure 2). Water level in the measured wells is listed in Table 1.

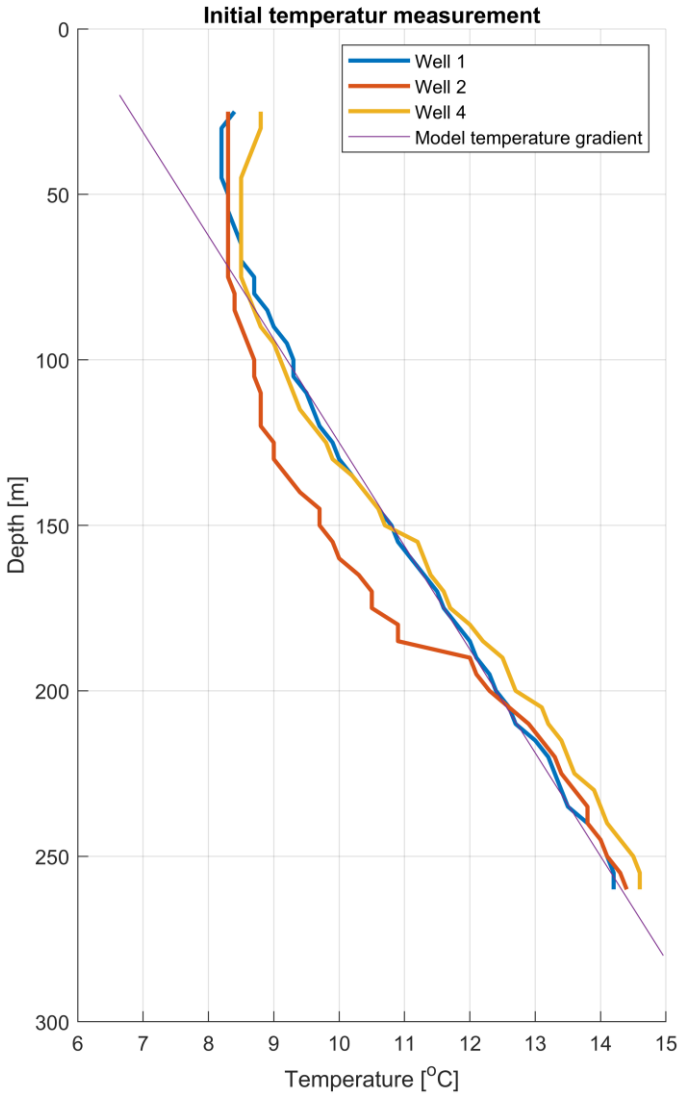


Figure 2. Temperature profiles for wells 1, 2, and 4. Annotated temperature gradient in figure is 3.2 °C/100 m with 6 °C at the surface.

Well	Depth [m]
1	23.6
2	22.8
4	20.4

Table 1. Measurement of water table in wells.

During the construction of the system, well 3 was prepared for experimental use and can be separated from the system. The downhole pipes can be accessed from above for temperature profile measurements when the brine is not circulating. Further, a second loop can be connected to the brine pipes in the well for experiments, circulating the brine in a separated loop (Figure 3). The system is prepared with temperature sensors and flowmeter for the brine pipes of well 3.

This offers two measurement conditions. One with the well disconnected where it is possible to measure the temperature profile for the full length of the well. The other with circulating brine, measuring temperature of brine down-flow, up-flow, and volume of circulated brine.

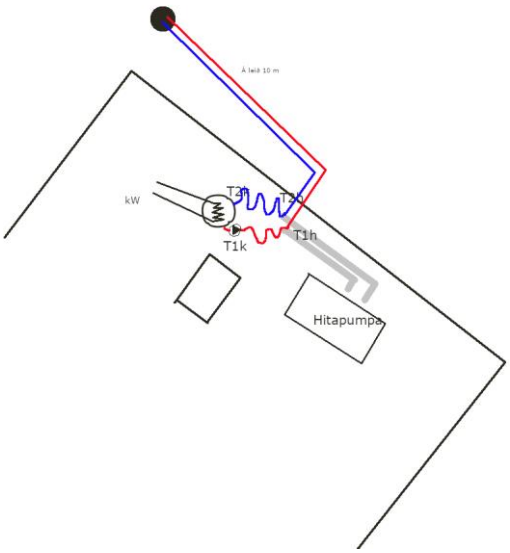


Figure 3. principle sketch of the experimental setup. Blue and red straight lines illustrate pipe from heat pump to geothermal well. Blue and red curled lines illustrate the rubber hose connecting the heater to the brine pipes. Black zigzag line inside circle represents the experimental heater system. Continuous measurement of the brine temperatures is on the brine pipes (T1h and T2h, Honeywell). Calibration measurements are on the heater system (T1k and T2k, Kamstrup). Electric power reader is on the electric supply connection.

The thermal response test is divided into one experiment where the heat recovery is measured from a steady state of consumption, followed by an experiment with thermal response in connection with heat storage.

Heat recovery from steady state conditions

After approximately one year of normal heat consumption, the heat recovery of the well was measured during one week. The temperature profile was measured for the full 400 m depth of the well at 5-m intervals. Typically, the measurement of the 80 data points for 400 m depth took between 15–20 minutes. The start time and end time is noted for each profile measurement. Figure 4 shows the measured temperature profiles.

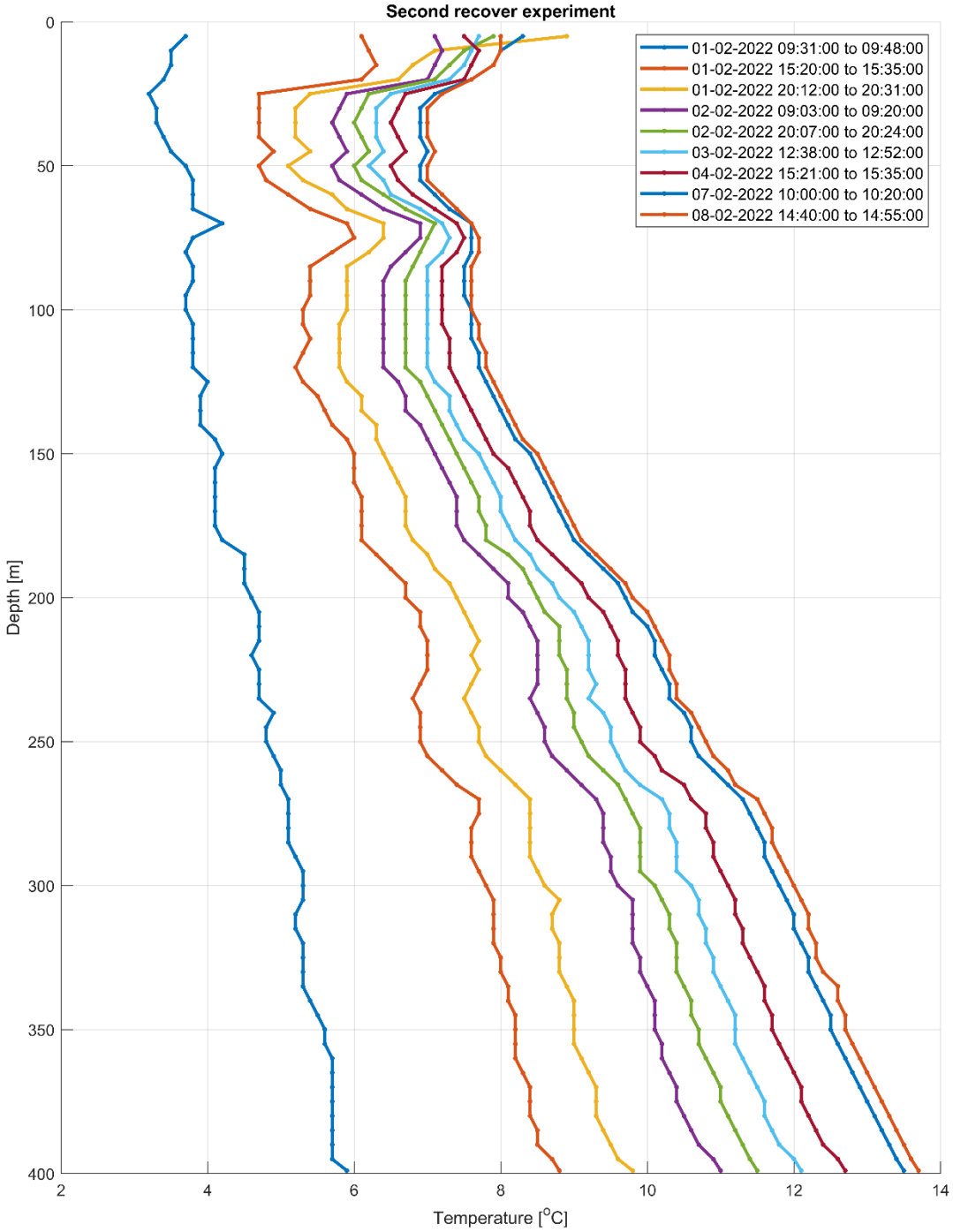


Figure 4. Temperature profiles during heat recover of the well. Legend shows the time intervals of measuring each temperature profile.

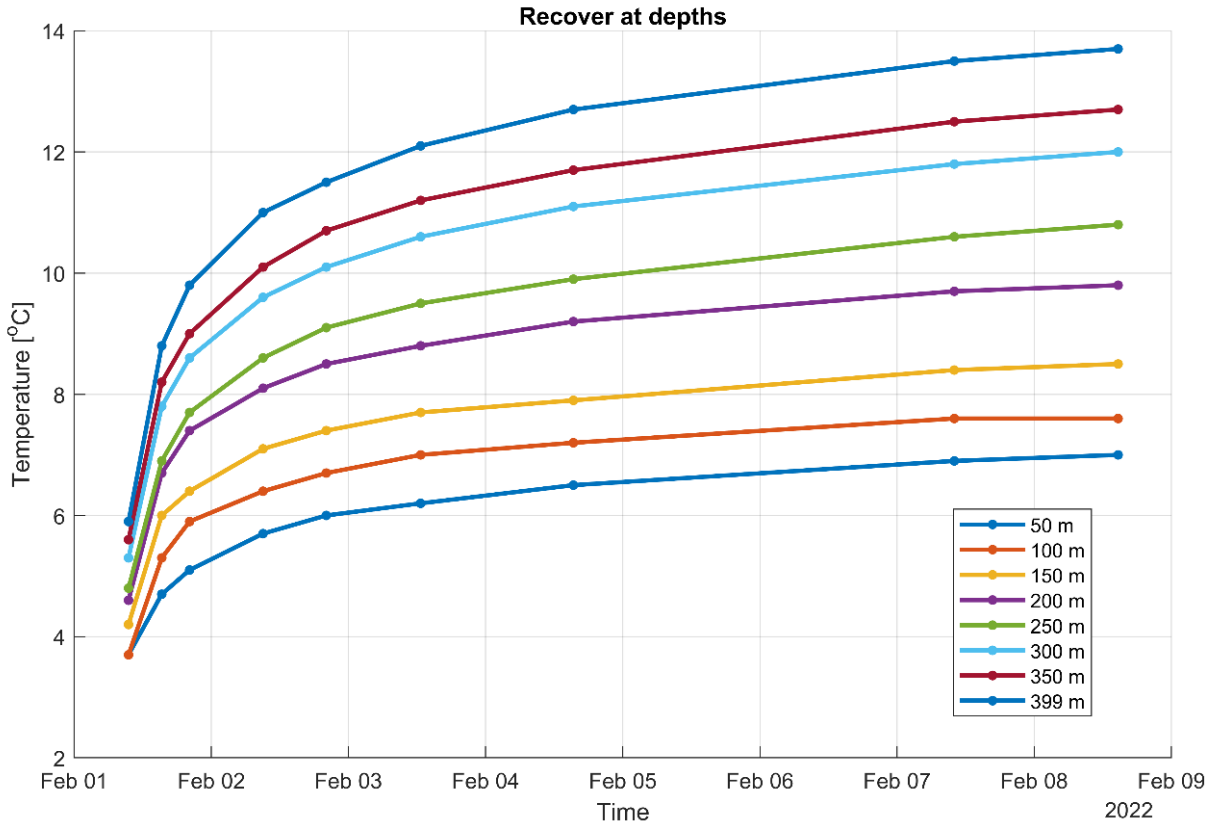


Figure 5. Time series of data in Figure 4 at selected depths. Legend shows depth of measurement in meters.

Heat storage experiments

From 9th February to 17th of March the well was back to normal consumption to establish steady state use-conditions.

The 17th of March the heat storage experiment was started. The experiment consists of:

Date	Status
17-03-2022 08:46	Stop brine circulation
17-03-2022 16:28	Start brine circulation, heater on
21-03-2022 22:01	Heater off, continue brine circulation
23-03-2022 08:47	Stop brine circulation
01-04-2022 06:49	Start brine circulation
01-04-2022 16:49	Heater on, continue brine circulation
03-04-2022 16:45	Heater off, continue brine circulation
05-04-2022 10:03	Stop brine circulation, stop experiment

Table 2. The sequence of the heat storage experiment.

The combined measurements are shown as time series in Figure 6 and temperature profiles in Figure 7.

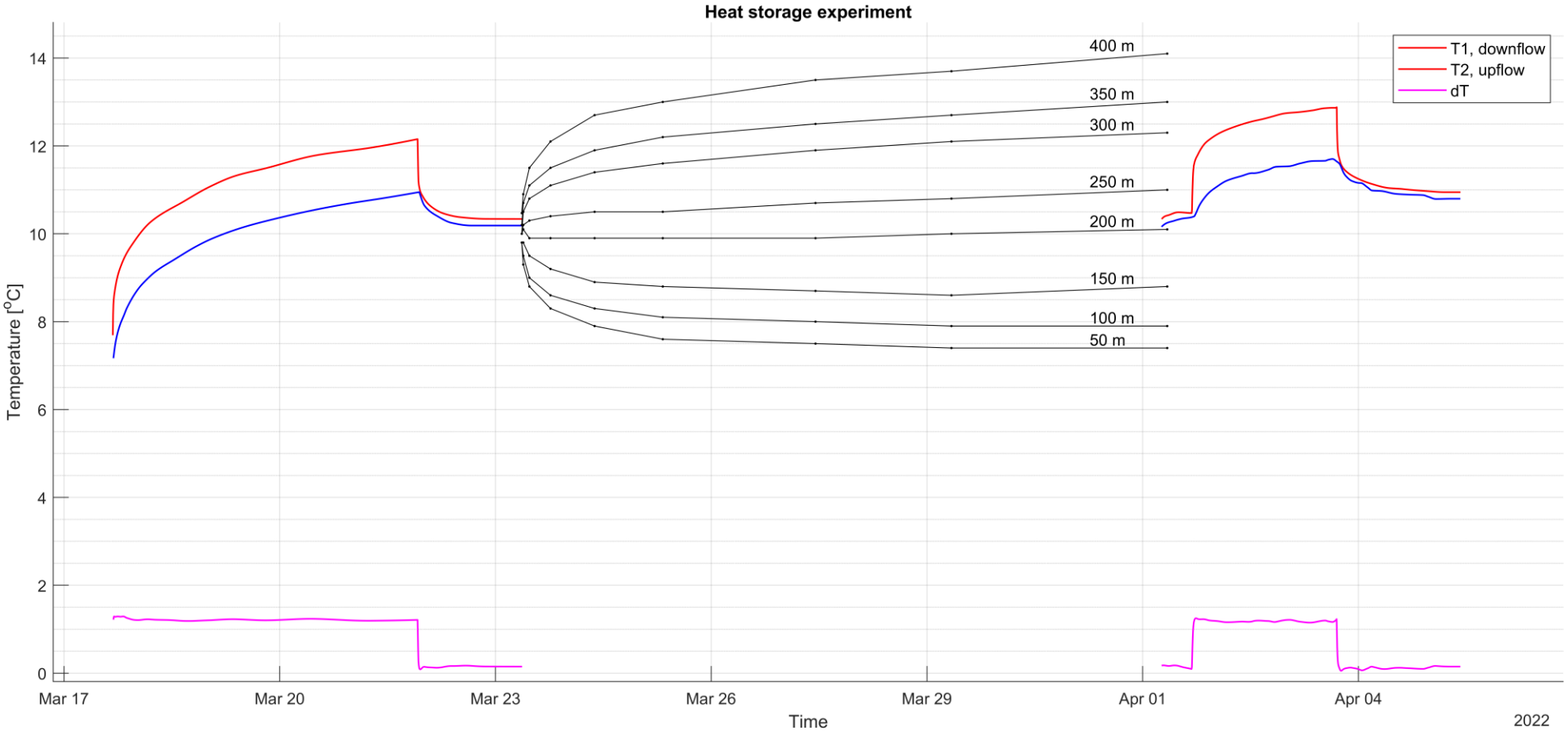


Figure 6.Recordings of brine temperatures, T1 down-flow and T2 up-flow. The temperature difference dT is calculated from T1 and T2. Black lines with dots show time series temperatures at fixed depths. Numbers show depth of measurements.

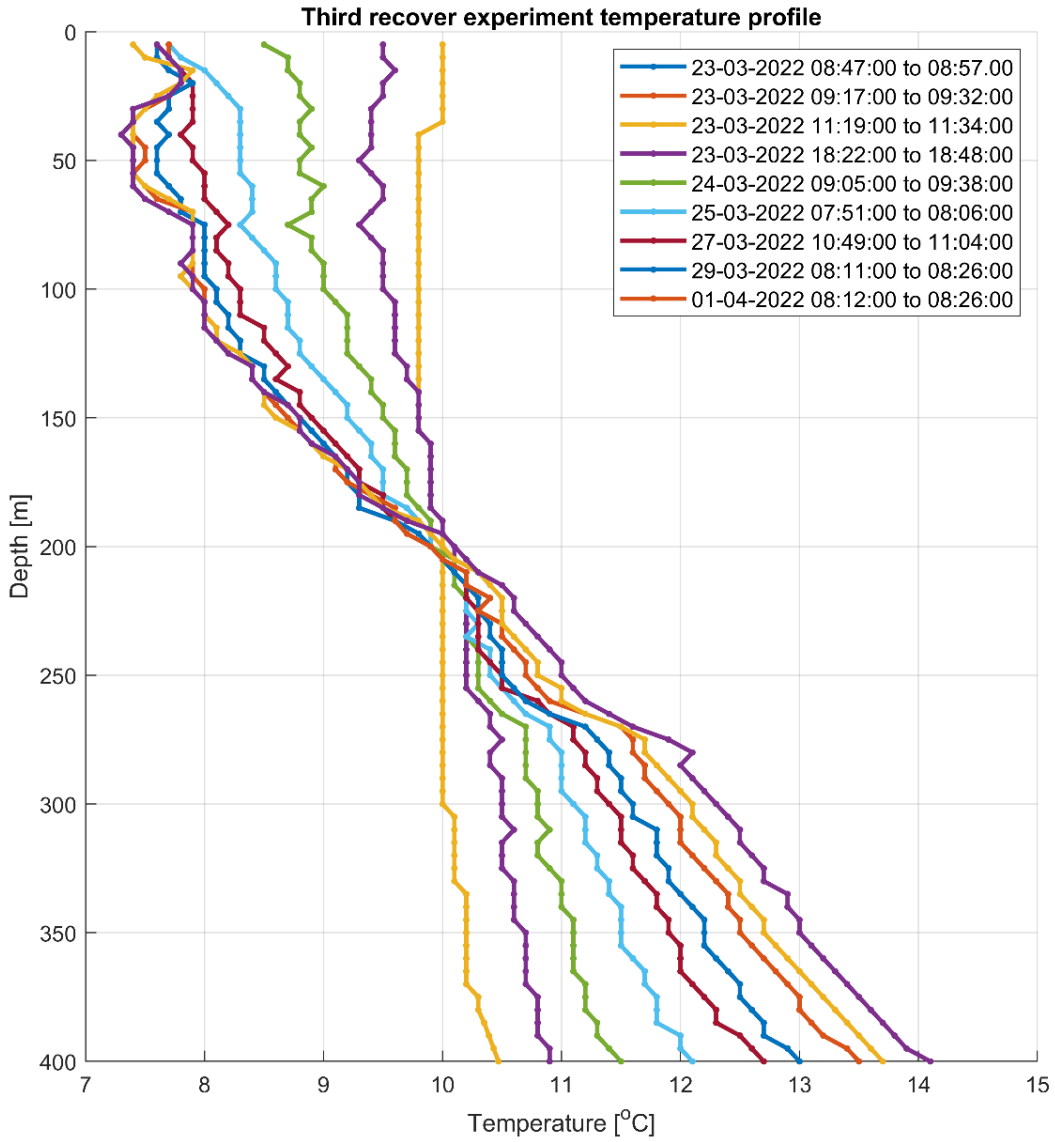


Figure 7. Temperature profiles during heat recover of well. Legend shows the time intervals of measuring each temperature profile.

3D numerical modelling

The modelling is based on Fourier's law of heat conduction (Equation 1) applied on a 3D model grid where each grid point is defined by individual heat capacity, head conductivity, and temperature (Figure 8).

$$q = -k\nabla T$$

Equation 1. Fouriers's law.

Fourier's law is considered to be an analogous to Ohm's law. Taking the analogy to Ohms law, the heat energy transmitted from one cell to the next is calculated between the centres of the two cells with a thermal resistance in between (Equation 2).

$$q = \frac{1}{R_{thermal}} dT = -\frac{kA}{l}\, dT$$

Equation 2. one dimensional case.

A is the surface connecting the two cells, *l* is the distance between the centre of the two cells, *k* is the thermal conductivity, and *dT* is the time step. For each time step the energy transmission is calculated for all cells and the temperature for each cell is calculated from the change in energy in the cells. For more details see Appendix A.

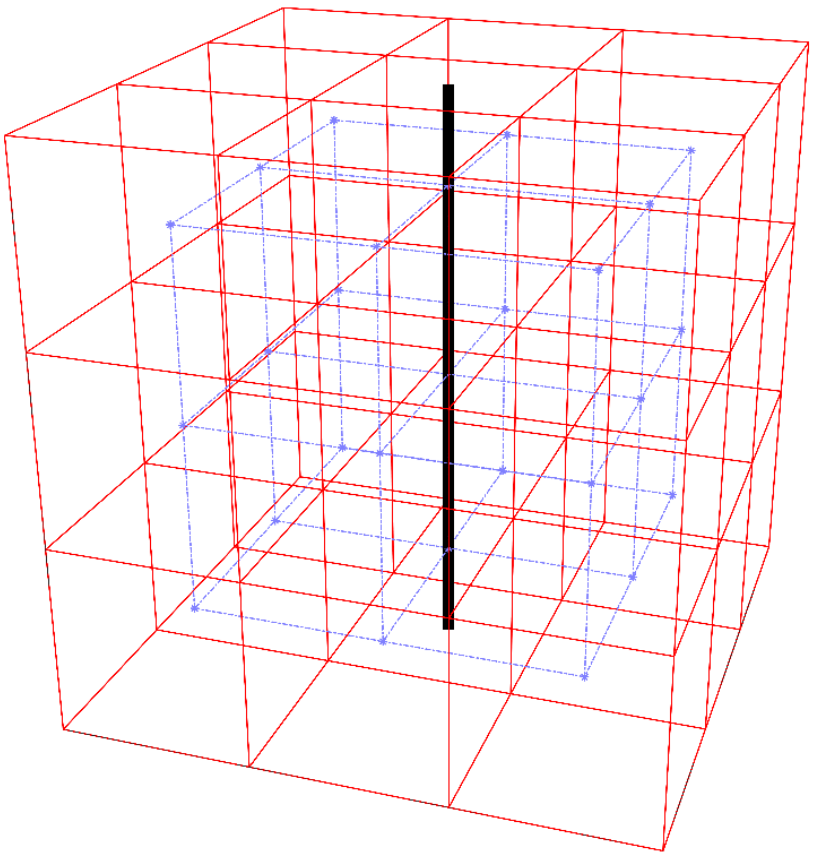


Figure 8. Example of a model grid showing centre points of grid cells (blue grid) and corner points of grid cells. The thick black line illustrates the geothermal well in the model.

Initial parameters

The initial temperatures for the model are derived from the temperature profiles measured just after completion of the drilling of the wells. The dominating trend of these profiles has a gradient of 3.2 °C /100m with 6 °C at the surface (Figure 2). The trend is derived from the temperatures in the 75–260 m interval and extended to the surface. Notice that 6 °C at the surface is close to the estimated surface temperature of 6.5 °C derived from all measurements of geothermal wells in the Faroes. From 0–75 m the gradient is close to zero with temperature of 8.5 °C and at about 20 m depth there is a temperature inversion with the temperature increasing from c. 8.5 °C to being c. 8.8 °C. The temperature profile for well 2 deviates from the two other wells in the 80–190 m interval as the water is colder in this interval. This could either be related to a downflow of water or to inflow of colder water at 190 m depth.

Based on this, the temperatures are assigned to the model with a vertical temperature gradient of 3.2 °C /100 m. From 75 to 20 m depth the temperature is constant at 8.5 °C and at 20 to 10 m it is 8.8 °C. In the uppermost 10 to 0 m the temperature is 6 °C.

The model is considered homogenous regarding heat capacity and conductivity, so all grid cells have been assigned the same value. The heat capacity *C* representative for basalt is between 2.4–2.6 [MJ/(m^3*°K)] (table 3.1 in Banks, 2008) using 2.52 [MJ/(m^3*°K)] for the modelling. The conductivity must be considered in relation to the geothermal heat flux. The geothermal flux is set to 60 mW/m^2 based on geothermal studies in the Lopra-1/1A well on Suðuroy (Balling, Breiner, & Waagstein, 2006). Based on geothermal flux the conductivity is 1.875 [W/(m*°K)] (Equation 3).

$$k = \frac{q \cdot l}{dT} = \frac{0.06 \cdot 100}{3.2} = 1.875\ [\frac{W}{m \cdot °K}]$$

Equation 3. Conductivity.

The first recover experiment (Figure 4) indicates that there is a flow of water crossing the well close to the surface and another flow at about 70–75 m depth. Both with temperatures that appear to converge towards the initial measured temperature profiles in Figure 2.

The hot water is considered to originate from the 290 m high mountain just south of the well locations, flowing in permeable layers transporting heat from inside the mountain to the surface. Several geothermal wells in the vicinity show similar temperature profiles with almost constant temperature close to 8 °C for the uppermost part of the wells.

The water flow is modelled as separate grids where, for each time step, the grid is moved one point in the flow direction to represent water flow. For each time step thermal equilibrium is assumed and heat is transferred between the grids accordingly. The flow rate is simulated by adjusting the heat capacity of the grid. The heat capacity necessary to model the observed heat anomalies is very small, less than 1 ‰ of the main grid. The modelling of flow is not intended to be quantified to the amount of water flowing but is intended to model the heat dynamics of the well. (Figure 9).

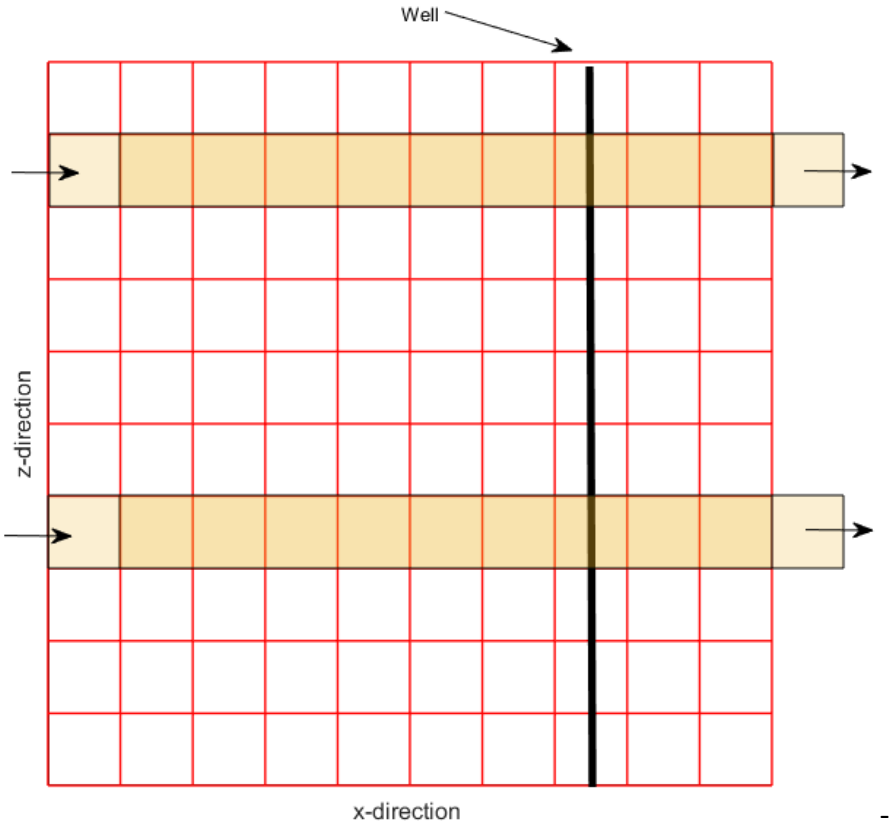


Figure 9.Principial model grid with 2 different layers simulating water flow as "water grids" being shifted on grid point at each time step.

Boundary conditions

The four vertical boundaries are modelled with no heat flux. The bottom boundary is modelled with the geothermal heat flux of 60 W/m^2. The top boundary should be modelled with heat flux determined from the combined incoming radiation from atmosphere and sun and the outgoing radiation from the surface. However, in this particular case, the temperature gradient is near zero in the uppermost ~75 m showing that the vertical heat flux in this part of the model is near zero. Therefore, at the top boundary, the heat flux is set to zero. Although there indeed is heat transmission at the top boundary of the model, it has none or little effect on the modelling since flow of hot water eliminates the effect.

Modelling geothermal well

The heat transmission in the geothermal well between the brine and the surrounding rock is a combined process of heat transmission from brine to water in the well, conduction and convection in water from brine pipes to rock wall, and transmission from water to rock. The brine down-flow and up-flow have different temperatures. Figure 10 a) shows an illustration of a cross section of the well.

This is in the modelling simplified to point-representation of the well, with an average temperature. The transmission is then determined from temperature difference between rock and brine and a transmission coefficient to be determined from the modelling (Figure 10 b)). By iterative analysis

the transmission coefficient of the modelled point-well is set to 250,000 [W/(m*°K)] for time steps of 3 hours. This parameter is of no physical significance and is only determined to achieve brine temperatures consistent with measurements.

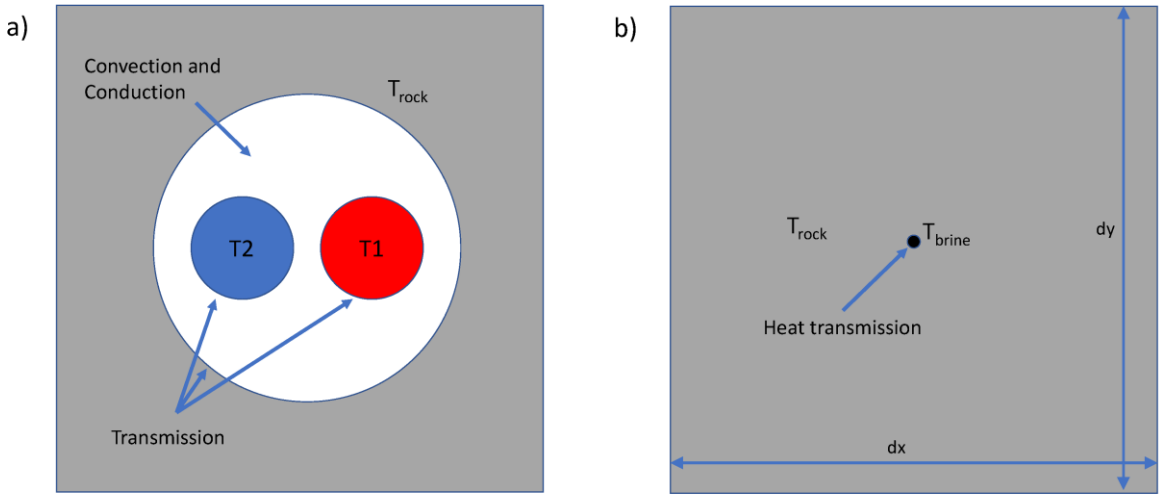


Figure 10. a) White circle: The water filled well, red circle T1: Down-flow of brine, blue circle T2: up-flow of brine, grey square: the surrounding rock, T_{rock}: temperature of the rock surrounding the well. b) dx and dy: horizontal size of the grids, T_{rock}: temperature of the grid point, T_{brine}: modelled average brine temperature, black dot: point representation of the well.

The modelling assumes constant average brine temperature for the full length of the well. Clearly T1 (down-flow) and T2 (up-flow) have temperature gradients, but whether the combined average temperature forms a constant temperature for the full length or is with a gradient, is a question.

It is not possible to measure the temperature profile in the well while the brine is circulating, but immediately after stopping circulation the temperature profile was measured by lowering the thermometer to the bottom at full speed. Nevertheless, it still takes 10 minutes to reach the bottom and within these 10 minutes the heat transmission from the rock will affect the brine temperature.

However, in this time interval, within 11 minutes from the stopping of circulation, the temperature profile is close to constant for the full length of the well. In the uppermost 150 m the temperature is 5.5 °C and at the bottom it is 5.5 °C. Between 150 m and the bottom it varies between 5.2 and 5.8 °C. Hence the approximation of constant average brine temperature appears to be valid for the modelling.

Modelling results

Model grid

First parameter to be established from the modelling is the grid size. Initial modelling was done with 1-m grids vertically and horizontally. The modelling is most sensitive to horizontal grid size, and in order to model the short-term dynamics consistent with measurements, a horizontal grid size of 0.2 m was necessary. A smaller grid of 0.15 m gave similar good results. Variations in vertical grid resolution had little impact. Grids of 1-m versus 5-m vertical resolution gave similar results.

The time scale of the modelling is about one year. For this a grid with total horizontal lengths of 40 m and depth of 500 m is considered adequate for a vertical geothermal well of 400-m depth. The horizontal grid number is 40/0.2=200 and the vertical grid number is 500/5=100. The total grid number of the model is 200*200*100=4.000.000.

The horizontal grid size of 0.2 m shall be seen in relation to that the well has a diameter of 0.112 m. 0.2 m is sufficient small compared to the well diameter to model the dynamics around the well to a certain degree.

The time step is determined from trial and set to 3 hours. At smaller time steps the modelling is instable.

Heat recovery experiment

The heat recovery experiments above are after approximately one year since the system was put to use.

To model the heat recovery, first the model was put in the state of one year heat consumption. The heat consumption during the year in use is not known. Therefore, several iterations were run to establish modelled results consistent with measurements in Figure 4 and 5. It was in this process that horizontal grid size of 0.2 m and vertical of 5 m was determined, and the transmission coefficient for the well. The modelled results of the heat recovery are shown together with measured values in Figure 11 and 12.

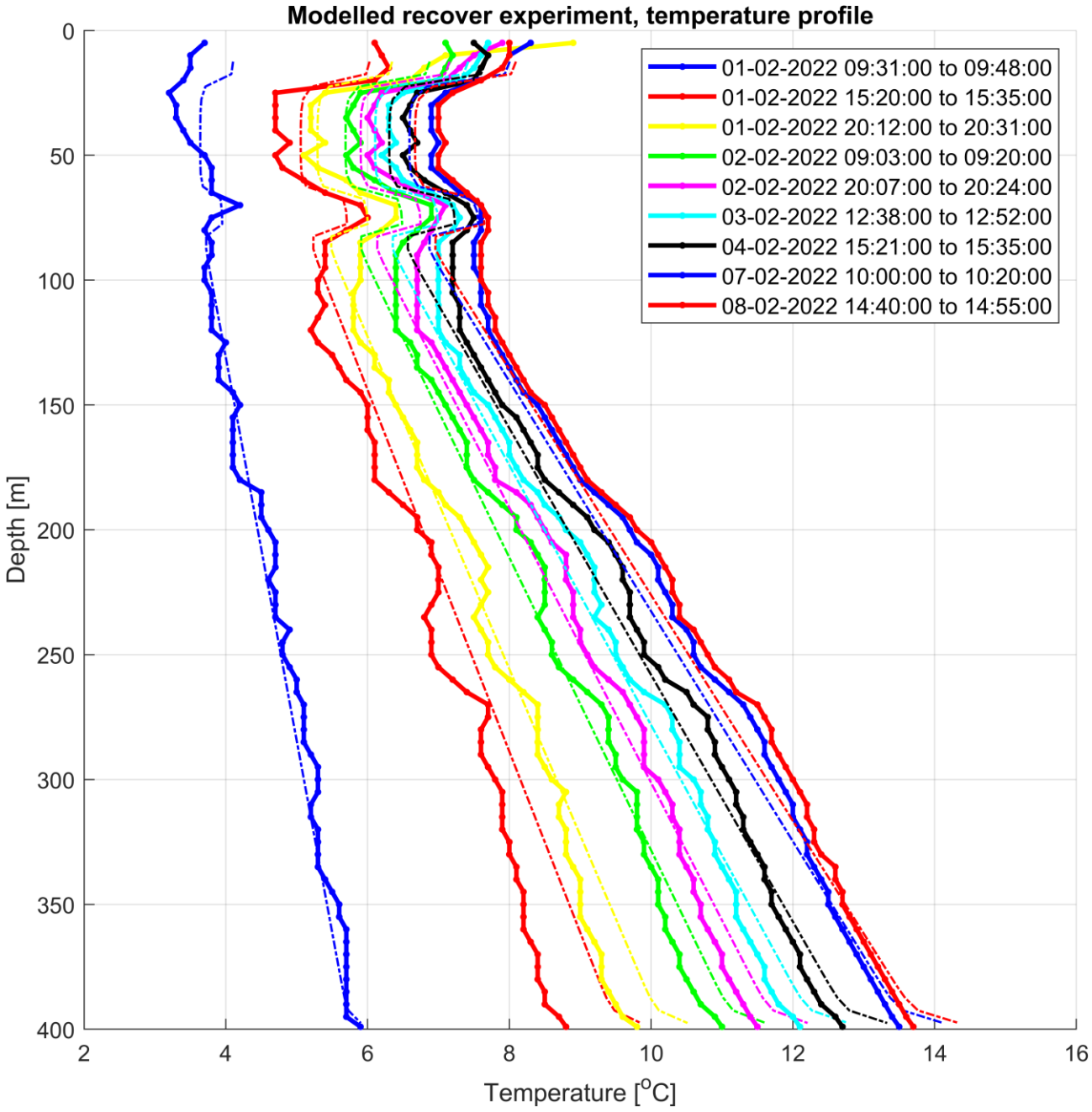


Figure 11. Modelled heat recovery of measurements in Figure 4. Thick lines how measurements and thin dotted lines show modelled values. Legend shows the time intervals of measuring each temperature profile.

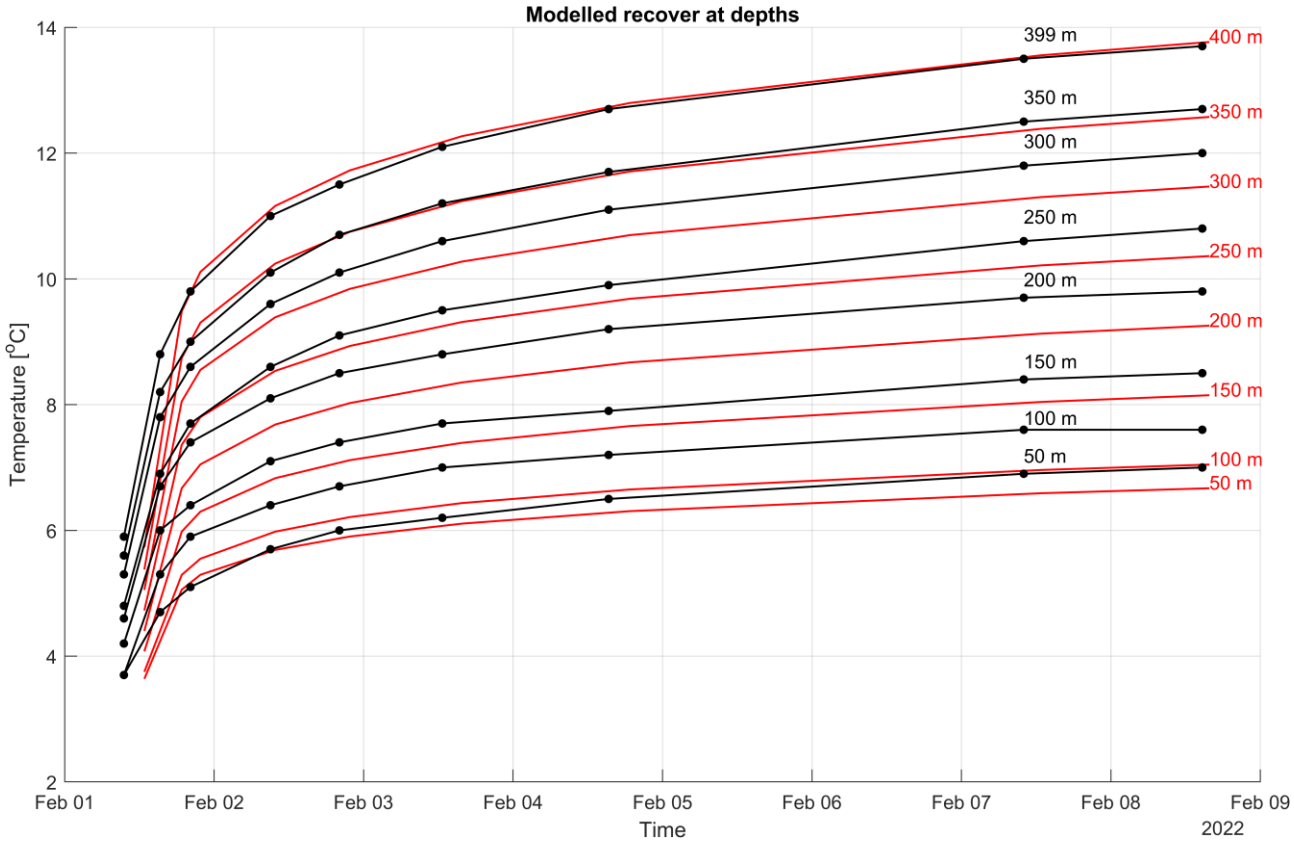


Figure 12. Modelled heat recovery of measurements in Figure 5 plotted in time series for different depths. Black point-lines show measurements and red lines show modelled values. Numbers show the depth in the well of the measurements.

Heat storage experiment

The heat storage experiment is modelled as a single sequence while applying the different conditions. The modelled results are plotted together with the measured values in Figure 13 and 14.

The heat capacity for 30% solution brine at 11 °C is about 4017251 [J/m^3*°K]. The measured flow is about 1.74 m^3/hour. The temperature difference of T1 and T2 is about 1.16 °C during heater on. The modelled heater power is thus 2250 W.

During heater off periods, there is also recorded a temperature difference between T1 and T2 of 0.15 °C representing heat power of 250 W, the origin of which is not known. However, the modelled values are much more consistent with observations when modelling heater power of 250 W in periods where the heater is off. There must be some heat exchange in the system while the brine is circulated from the well through brine pipes, through hoses through the external heater system, and back to the well, although the heater is off.

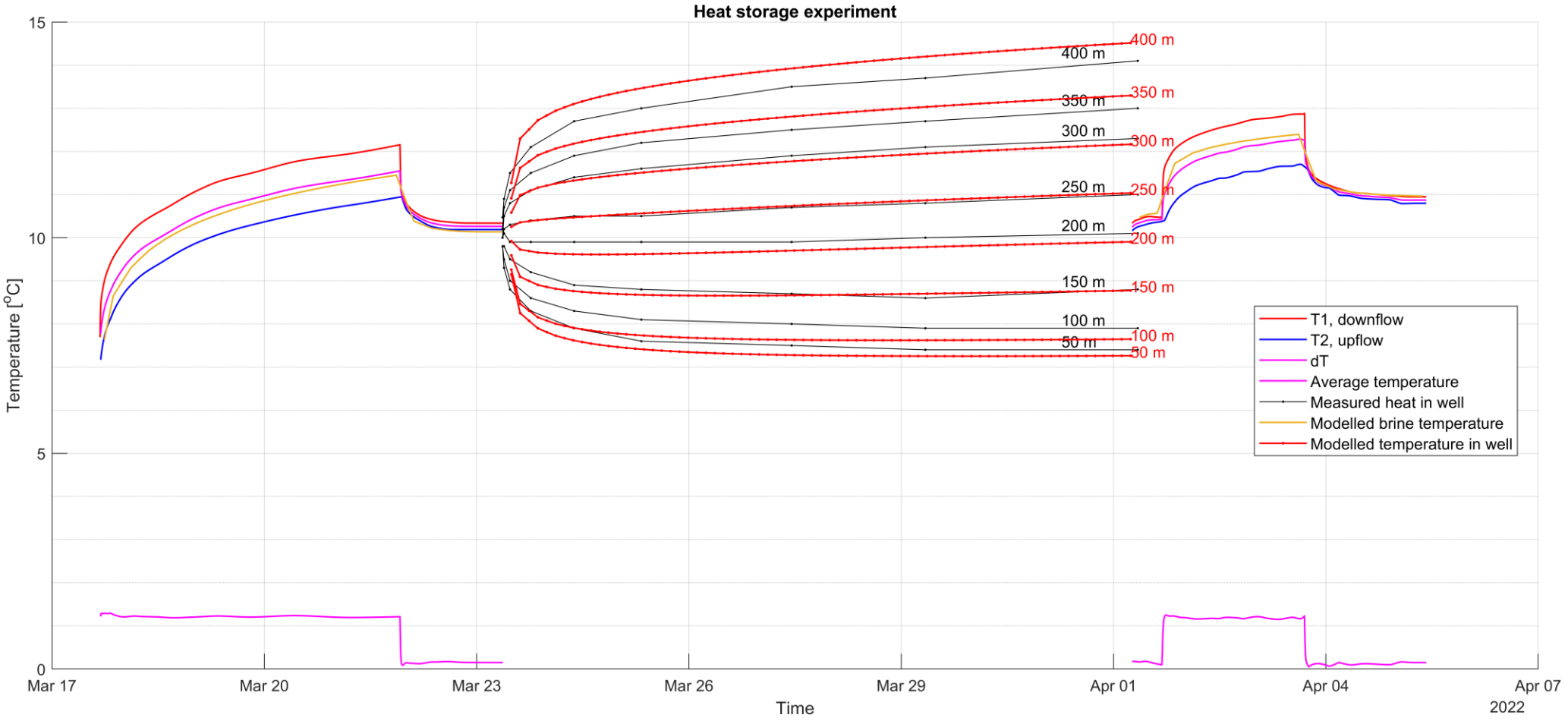


Figure 13. Same as Figure 6 but with modelled results added. In addition to measured T1 and T2, a calculated average brine temperature is added to be compared directly to the modelled average brine temperature. Numbers show depth of measurements.

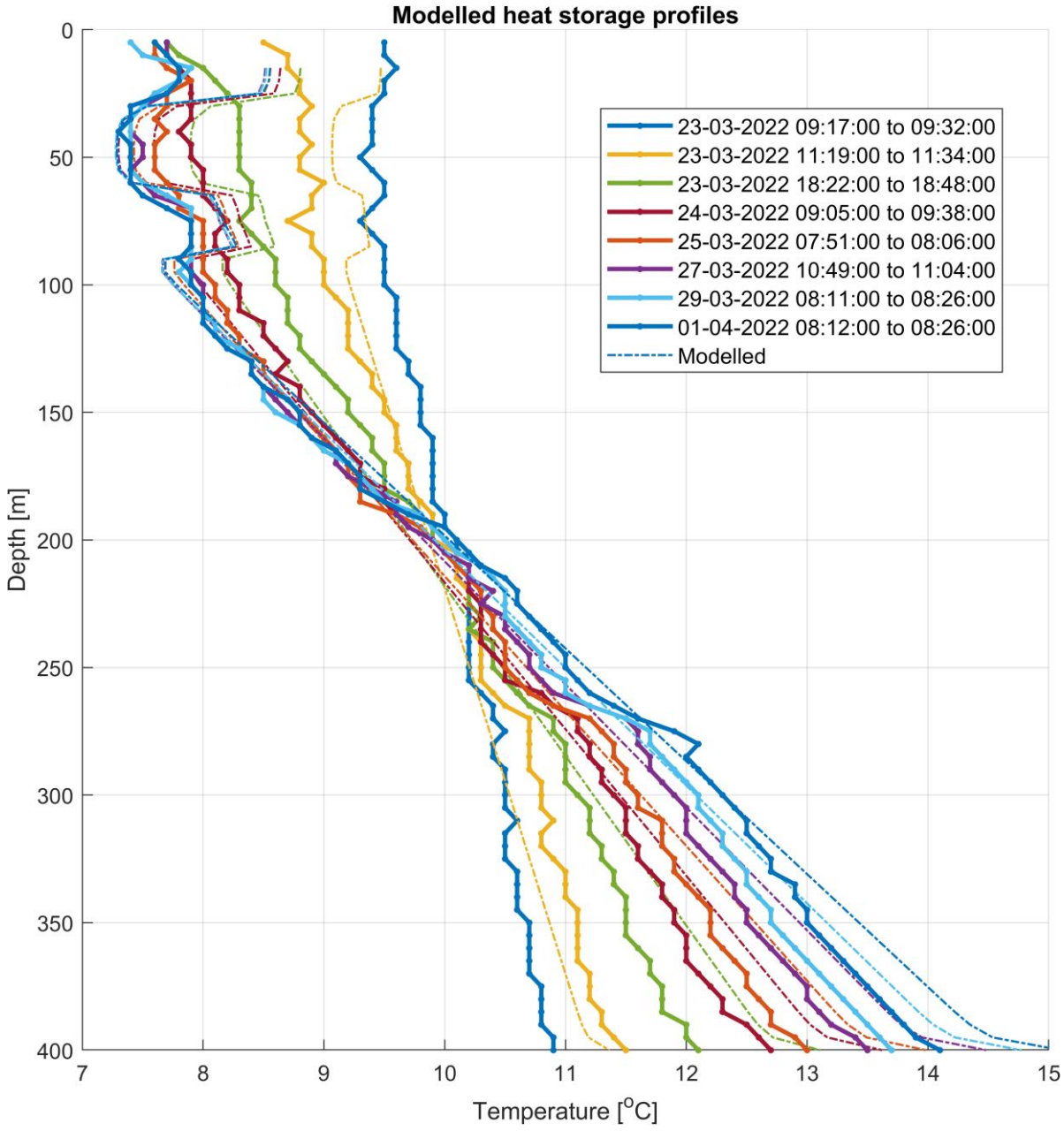


Figure 14. Modelled heat recovery of measurements in Figure 7. Thick lines show measurements and thin dotted lines show modelled values. Legend shows the time intervals of measuring each temperature profile.

Conclusion on modelling performance

Based on the results from the 3-weeks continued modelling with varying operating conditions, the model has been verified for this timescale of operation (Figure 13).

For the one-year condition there is the uncertainty of the actual heat load during this period. However, the model exhibits a heat recovery after one year of use that is consistent with observations (Figure 11).

The anomalies of the temperature gradient in the uppermost 100 m of the well are to a certain degree reproduced by assumption of flow of water in 2 layers. The amount of water flow has not been established, although it is in small quantities.

There are smaller deviations from a constant temperature gradient in the lower part of the well, but there has been no attempt to model these. They are expected to originate from variations of rock properties or minor water flow or a combination of this.

The determining of the conductivity is based on the assumption that the geothermal heat flux in the Lopra-1/1A well of 60 mW/m^2 is also valid for the well at Umhvørvisstovan, Tórshavn. Different values of the conductivity will affect the estimation of heat consumption during one year of load and the transmission coefficient of the modelled well. Further tests with a range of conductivity values are recommended.

However, although there are uncertainties regarding the specific modelling of the well, the comparison with measured values shows that the model exhibits the heat response dynamics observed in the test-well and is thus a useful tool in the analysis of different operations conditions of geothermal wells in the Faroe Islands.

Future work

Geothermal heating of housing is in rapid development these years in the Faroes. For Many of the geothermal wells the initial temperature profile has been measured by Jarðfeingi. It is well documented that well-conditions can vary with colder areas, warmer areas, wells with artesian relative hot water, wells with relative cold downflowing water, wells with high water table, and wells with low water table. The impact of the different conditions on the operation efficiency is not well described and considering the ongoing huge investments in the field, access to better advice would be desirable. Seen from the consumers point, it is of great interest how the difference in conditions affects the rentability of the system and the long-term temperature development of the well.

The current modelling is a step in that direction and can be developed further to address all of the conditions listed above. Further, it can, based on time data series of the brine temperatures for a system together with the load condition, give information on the condition of a geothermal well in operation.

The modelling can also be developed to model the effect of having the up-flow brine pipe insulated, such that the upcoming heat energy is not deposited in the upper part of the well, providing higher brine temperature to the heat pump.

And finally, most important in connection with this project, the modelling can be used to predict the effect of storing excess energy in geothermal wells. However, before this can be addressed, the setup in question must be defined.

When storing waste heat in geothermal wells, the energy will be stored at the temperature of the well. That is, although the temperature of the heat is above 20 °C it will be stored at about 5 °C. This is a major deterioration of the quality of the heat, and it is expected to be regained as only a very slight, insignificant improved COP. Which leads to that the main contribution of storing waste heat in geothermal wells, is to extend the lifetime of the well.

However, if the energy to be stored is from excess electric power from windmills, separate wells, only intended for high temperature storage might be considered. It could be considered to make further experiments, storing high temperature energy in the well. This would, however, require long-time experiments, in the order of years, with high power heater. The energy cost would be in the order of millions DKK.

It is in this context that the developed modelling has its value. With 3D modelling of the heat dynamics, it will be possible to predict the general behaviour of high-temperature heat storage, and thereby come closer to a conclusion on, to what degree it is a feasible method to recover excess energy.

References

Balling, N., Breiner, N., & Waagstein, R. (2006). Thermal structure of the deep Lopra-1/1A borehole in the Faroe Islands. In J. A. Chalmers & R. Waagstein (Eds.), *Scientific results from the deepened Lopra-1 borehole, Faroe Islands* (Vol. 9, pp. 91-108): Geological Survey of Denmark and Greenland Bulletin.

Banks, D. (2008). *An Introduction to the Thermogeology*: Blackwell Publishing Ltd, 9600 Garsington Road, Oxford OX4 2DQ, UK.

Appendix A

3D numerical modelling

The numerical modelling is based on Fourier's law (Equation 4).

$$q = -k\nabla T$$

Equation 4

The model is gridded.
The ith cell is defined by length (dx_i), width (dy_i), and higth (dz_i).
Fourier's law is considered to be analogous to Ohm's law (ref?).
Taking the analogy to Ohms law, the heat energy transmitted from one cell to the next is calculated between the centres of the two cells with a thermal resistance in between.

$$q = \frac{1}{R_{thermal}} dT = -\frac{kA}{l}\, dT$$

Equation 5. one dimensional

dT is the temperature difference between the two cells.
When the two adjacent cells have different conductivity and the dimensions of the cells differ, the combined thermal resistance is calculated as

$$\frac{1}{R} = \frac{1}{R' + R''} = \frac{1}{\frac{l'}{k'A} + \frac{l''}{k''A}} = \frac{A}{\frac{l'}{k'} + \frac{l''}{k''}} = \frac{k'k''A}{l'k'' + l''k'}$$

Equation 6

The transmitted energy from one cell to the other between is then

$$q = \frac{1}{R_{thermal}} dT = -\frac{k'k''A}{l'k'' + l''k'}\, dT$$

Equation 7

The expression of the transmitted energy in one dimension from right to cell *i* is

$$q_i = -\frac{k_i k_{i+1} A_i}{l_i k_{i+1} + l_{i+1} k_i} (T_i - T_{i+1})$$

Equation 8

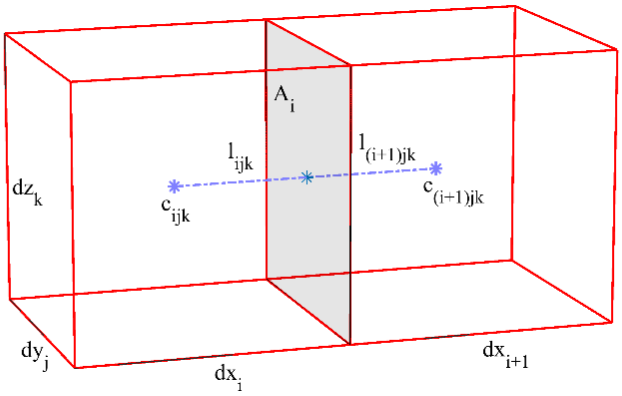


Figure 15. Illustration of parameters l_i and A_i used in Equation 8. The equation only considers one dimension while the figure considers 3 dimensions hence l_i is l_{ijk} in the figure. c_{ijk} is the centre point of the grid cell.

qi: heat flux [W]
k_i: conductivity of the i^{th} cell [W/mK].
l_i: distance from centre to face in direction of the transmitted energy of the i^{th} cell [m].
A_i: area transmitting the energy, $A_i = dy_i \times dz_i$ [m^2].
T_i: Temperature of i^{th} cell [K].

The energy transmitted in each time interval Δt is

$$\Delta Q_i = -\frac{k_i k_{i+1} A_i}{l_i k_{i+1} + l_{i+1} k_i} (T_i - T_{i+1}) \Delta t$$

After each timestep the energy of the cell is updated, and the new temperature of the cell is calculated.

$$Q_i(t + \Delta t) = Q_i(t) + \Delta Q_i$$

Equation 9

$$T_i(t + \Delta t) = \frac{Q_i(t + \Delta t)}{C_i} = \frac{Q_i(t) + \Delta Q_i}{C_i}$$

Equation 10

C_i is the heat capacity of ith cell.

The above is implemented in Matlab calculating transmitted energy in both directions for all three dimensions. In an arbitrary large grid and with arbitrary vectors defining dx, dy, and dz although the grid number of the model is a limitation depending on RAM size of the computer.

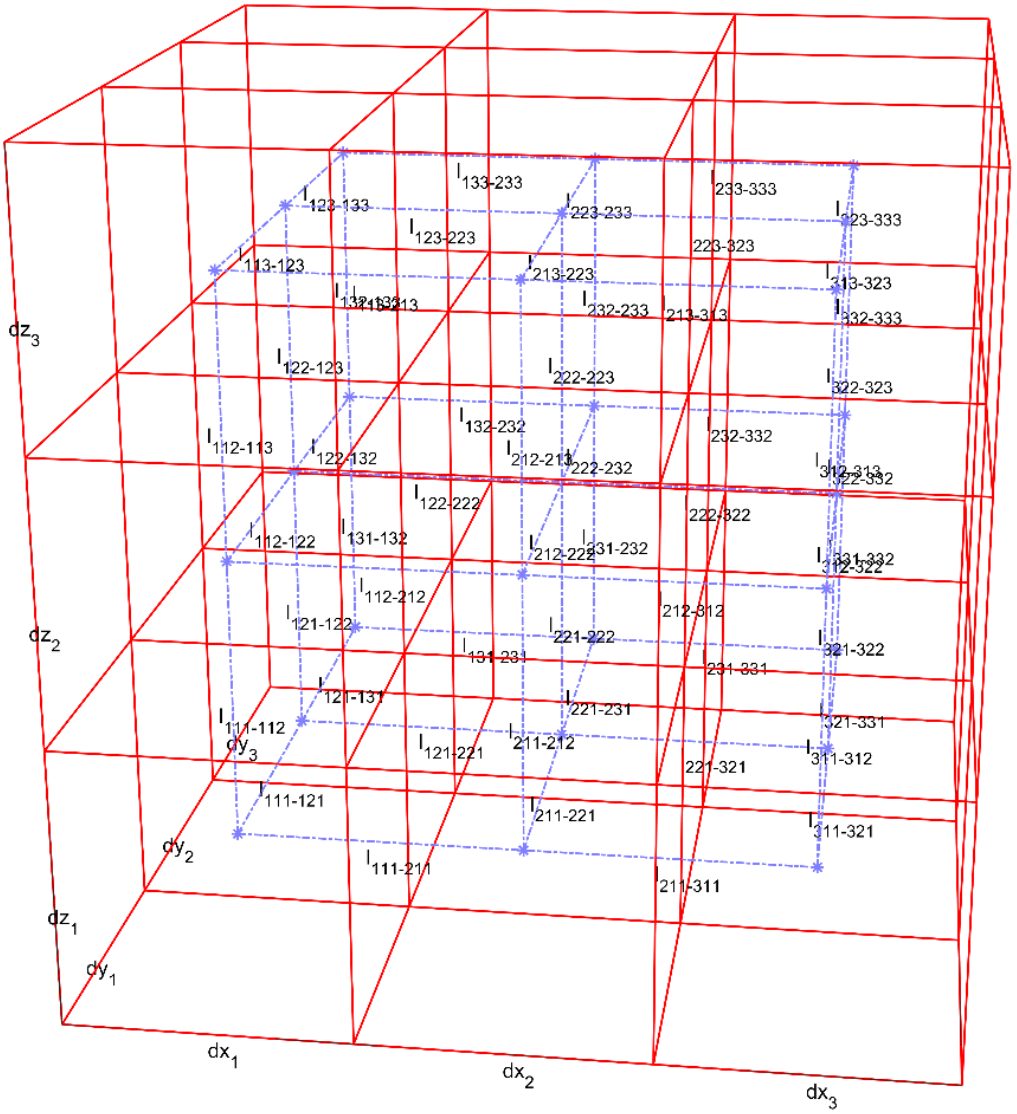


Figure 16. The vectors dx, dy, and dz, define the gridding of the model. The energy of each cell is considered to be at a source point (mass mid-point) at the centre of each cell.

Instability criterion

Sizes of dx, dy, dz, and dT must be considered in relation to instability criterions.

(https://en.wikipedia.org/wiki/Von_Neumann_stability_analysis)

If the errors decay and eventually damp out, the numerical scheme is said to be stable.

$$r = \frac{\alpha \Delta t}{(\Delta x)^2} \leq \frac{1}{2}$$